

Construction of a full-thickness human corneal substitute from anterior acellular porcine corneal matrix and human corneal cells

Kai Zhang^{1,2}, Xiao-Xiao Ren¹, Ping Li¹, Kun-Peng Pang³, Hong Wang⁴

¹Department of Ophthalmology, Shandong Provincial Western Hospital, Jinan 250022, Shandong Province, China

²Shandong Institute of Otolaryngology, Jinan 250022, Shandong Province, China

³Department of Ophthalmology, Qilu Hospital, Shandong University, Jinan 250012, Shandong Province, China

⁴Department of Ophthalmology, Shandong Provincial Hospital Affiliated to Shandong University, Jinan 250021, Shandong Province, China

Correspondence to: Hong Wang, Department of Ophthalmology, Shandong Provincial Hospital Affiliated to Shandong University, No.4, Duanxing West Road, Jinan 250021, Shandong Province, China. wanghong630223@163.com

Received: 2018-06-27 Accepted: 2018-11-28

Abstract

• **AIM:** To construct functional human full-thickness corneal replacements.

• **METHODS:** Acellular porcine corneal matrix (APCM) was developed from porcine cornea by decellularization. The biomechanical properties of anterior-APCM (AAPCM) and posterior-APCM (PAPCM) were checked using uniaxial tensile testing. Human corneal cells were obtained by cell culture. Suspending ring was designed by deformation of an acupuncture needle. MTT cytotoxicity assay was used to check the cytotoxicity of suspending ring soaking solutions. A new three-dimensional organ culture system was established by combination of suspending ring, 48-well plate and medium together. A human full-thickness corneal substitute was constructed from human corneal cells with AAPCM in an organ coculture system. Biochemical marker expression of the construct was measured by immunofluorescent staining and morphological structures were observed using scanning electron microscopy. Pump function and biophysical properties were examined by penetrating keratoplasty and follow-up clinical observations.

• **RESULTS:** There were no cells in the AAPCM or PAPCM, whereas collagen fibers, Bowman's membrane, and Descemet's membrane were retained. The biomechanical property of AAPCM was better than PAPCM. Human corneal cells grew better on the AAPCM than on the PAPCM.

There was no cytotoxicity for the suspending ring soaking solutions. For the constructed full-depth human corneal replacements keratocytes scattered uniformly throughout the AAPCM and expressed vimentin. The epithelial layer was located on the surface of Bowman's membrane and composed of three or four layers of epithelial cells expressing cytokeratin 3. One layer of endothelial cells covered the stromal surface of AAPCM, expressed Na⁺/K⁺ATPase and formed the endothelial layer. The construct was similar to normal human corneas, with many microvilli on the epithelial cell surface, stromal cells with a long shuttle shape, and zonula occludens on the interface of endothelial cells. The construct withstood surgical procedures during penetrating keratoplasty. The corneal transparency increased gradually and was almost completely restored 7d after surgery.

• **CONCLUSION:** AAPCM is an ideal scaffold for constructing full-thickness corneal replacement, and functional human full-thickness corneal replacements are successfully constructed using AAPCM and human corneal cells.

• **KEYWORDS:** full-thickness human corneal substitute; anterior-acellular porcine corneal matrix; posterior-acellular porcine corneal matrix; human corneal cells

DOI:10.18240/ijo.2019.03.01

Citation: Zhang K, Ren XX, Li P, Pang KP, Wang H. Construction of a full-thickness human corneal substitute from anterior acellular porcine corneal matrix and human corneal cells. *Int J Ophthalmol* 2019;12(3):351-362

INTRODUCTION

Second only to cataracts, corneal disease is the most frequent cause of vision loss^[1]. There are more than 50 million people worldwide who have suffered vision loss due to corneal opacification because of disease or trauma^[2]. The keratoplasty is widely used to treat corneal blindness^[3-5]. However, the source of acceptable donor corneal tissue is limited, especially in developing countries^[6]. Furthermore, this situation is becoming more serious because of the increasing use of corrective corneal laser vision surgery and the rising incidence of transmissible diseases, such as HIV and hepatitis^[7-9].

At present, keratoprotheses are the sole substitutes for donor corneas in keratoplasty. However, they are associated with serious complications, including retroprosthetic membrane formation, neovascularization, infection, and glaucoma. Thus, their use in the clinic has been strictly limited^[10]. In addition, according to European directives many laboratory animals are not allowed to use for toxicity testing, particularly the rabbits that were previously used in the Draize eye irritancy test^[11]. Therefore, it is necessary to develop tissue-engineered corneas that can replace donor corneas for keratoplasty and animal models in pharmacotoxicology testing.

The human cornea is a transparent and multilayered tissue composed of three distinct layers, each consisting of a different cell type. The corneal epithelium, comprising stratified squamous epithelial cells, is the outermost layer^[12]. It is responsible for protecting the eye from physical agents and transporting oxygen and nutrients to the deeper layers of the cornea.

The corneal stroma consists of approximately 200 lamellae and its thickness is about 500 μm , accounting for 90% of the whole corneal thickness. The lamellae appears as a highly organized array of collagen I fibrils that lie parallel to each other and small, populating keratocytes with a uniform diameter that are quiescent and dispersed between the fibrils to maintain the extracellular matrix, which is essential for transparency^[13-17]. The orientation of array of lamellae changes sharply, coming into a plywood-like organization that provides stability to the cornea and gives it its biomechanical properties. The damaged stroma is replaced by fibrotic tissues because of its non-regenerated property^[18-19]. Finally, the endothelial cell layer consists of a single layer of regularly arranged hexagonal cells [*i.e.* corneal endothelial cells (CECs)] and separates the corneal stroma from the aqueous humor of the anterior chamber. The liquid balance within the cornea is maintained by the barrier and compensating pump functions of the CECs, which is critical for corneal transparency^[20]. Thus, only to develop all three layers of the cornea can a corneal equivalent be obtained. Many researchers have developed several full-thickness human corneas^[18,21-23] and hemicorneas^[24-27] using natural or synthetic polymers and normal human corneal cells or immortalized cells, which have been used primarily for *in vitro* drug and toxicity testing, based on their delicate mechanical properties, and in biosafety studies for corneal transplantation.

Recently, we developed a new scaffold named acellular porcine corneal matrix (APCM), which was derived from porcine cornea^[28] and CEC-like cells derived from human embryonic stem cells (hESCs)^[29-30]. We successfully constructed rabbit anterior hemicorneas and human posterior hemicorneas using anterior APCM (AAPCM) and rabbit corneal cells, posterior acellular porcine corneal matrix (PAPCM), and hESC-derived CEC-like cells and used them for rabbit lamellar

and endothelial keratoplasty, respectively^[29-32]. However, the biofunction, biosafety, and biocompatibility of these constructs *in vivo* should be evaluated before they are introduced into the clinic. The studies above demonstrated that APCM has good biocompatibility and biomechanical properties and that the characteristics of hESCs-derived CEC-like cells are similar to those of native human CECs. In this regard, it is unknown whether bare APCM can be used to construct full-thickness corneas and whether corneal replacements that are constructed from APCM can withstand surgical procedures during penetrating keratoplasty, especially resisting stitches and the intraocular pressure after transplantation.

In this study, we constructed a full-thickness human corneal replacement with anterior APCM lamellae, normal human keratocytes, epithelial cells, and hESC-derived CEC-like cells. We found that it had better biomechanical properties than a replacement constructed with posterior APCM in a new three-dimensional organ culture system that we designed using a special suspending ring.

MATERIALS AND METHODS

Ethical Approval This research was approved by the Institutional Review Board of Shandong Provincial Western Hospital. Treatment is in full compliance with the ARVO Statement for the Use of Animals in Ophthalmic and Vision Research. Samples were collected following written informed agreements, and the study was implemented according to the Declaration of Helsinki.

Cell Culture Human epithelial and stromal cells were obtained from a human donor limbal rim, which was not adequate for transplantation. The human limbal rim was incubated with 2.4 U/mL Dispase II (Roche, Basel, Switzerland) at 37°C for 1h after rinsing three times with DMEM/F12 (Invitrogen, Waltham, MA, USA). Two fine forceps were used to separate the limbal epithelial sheets from the human limbal rim under a dissecting microscope. Single cells were obtained by digesting the limbal epithelial sheets with 0.25% Trypsin/0.02% EDTA (Sigma, Darmstadt, Germany) at 37°C for 5min.

The human donor cornea was deprived of epithelial and endothelial cells and residual stroma was chopped into small pieces of approximately 1.0 mm in diameter, which were digested into single cells with 0.02% collagenase (Sigma).

DMEM/F12 (1:1) supplemented with 10% fetal bovine serum (Invitrogen, Waltham, MA, USA), 100 U/mL penicillin and 100 U/mL streptomycin was used as a growth medium for the epithelial and stromal cells.

The method for the derivation of CEC-like cells from hESCs was used as reported previously^[30]. The basal medium (BM) contained DMEM/F12 (Invitrogen, Waltham, MA, USA) supplemented with B27 (Invitrogen), 20 ng/mL epidermal growth factor (Sigma), 40 ng/mL basic fibroblast growth factor

(Sigma), 100 U/mL penicillin and 100 U/mL streptomycin (Shandong Lukang Pharmaceutical co., Ltd, Jining, China). Then, 10% fetal bovine serum was added to BM to form corneal fibroblast differentiation medium (FM). Lens epithelial cell-conditioned medium was mixed with FM at a ratio of 3:1 as the CEC differentiation medium (EM). Embryonic bodies (EBs) were formed and cultured in suspension for 7d with hESC growth medium in low-attachment culture dishes. The isolated human corneal stromal cells (hCSCs) were plated at $1800/\text{cm}^2$ onto 0.4-mm-pore transwell inserts (Corning) and cultured in FM. Approximately 80 EBs per well were plated onto 10 mg/mL fibronectin-10 mg/mL laminin-10 mg/mL heparan sulfate-precoated, 24-mm-diameter glass cover slips in wells of a 6-well tissue culture plate and cultured in BM for 2d. Subsequently, the hCSCs on transwell inserts were added to the 6-well plates and cocultured with the plated EBs in FM for an additional 5d with changes in medium every 2d. Then, the medium was changed from FM to EM and culturing was continued for 2wk. Cells with N-cadherin and vimentin double staining were CEC-like cells. All cultures were performed in a Carbon dioxide cell incubator containing 5% CO_2 at 37°C.

Preparation of Anterior APCM and Posterior APCM
Decellularization of porcine corneas was implemented according to the previous protocols in our lab^[28]. A 1.0-mm thick, 10.0-mm diameter APCM containing Bowman's membrane and anterior stromal collagen (*i.e.* AAPCM) or posterior stromal collagen and Descemet's membrane (*i.e.* PAPCM) was prepared using a scalpel under a dissecting microscope. AAPCM and PAPCM were washed three times in sterile phosphate buffer saline (PBS) supplemented with 200 U/mL penicillin and 200 U/mL streptomycin for 3h, freeze-dried at -20°C for 12h, air-dried at room temperature for 3h in a biological safety cabinet, and stored at -20°C before use. All steps were accomplished under aseptic processing procedures.

Reformulation of Corneal Epithelium and Endothelium on AAPCM and PAPCM
AAPCM and PAPCM lamellae were soaked in EM at 37°C for 24h. Subsequently they were placed in individual wells of 48-well plates. The CECs from passage 1 were gently seeded onto the surface of the Bowman's membrane of AAPCM and stoma of PAPCM with a cell density of $5 \times 10^3/\text{mm}^2$ and cultured for 7d. When epithelial cells grown to reach confluence, the air-liquid culture technique was used for one more week for the construction of epithelium. For the construction of endothelium, CEC-like cells in 100 mL were gently seeded on the surface of the stoma of AAPCM and Descemet's membrane of PAPCM at a density of 2×10^5 cells/ mm^2 for each lamella, and then allowed to adhere for 4h before being completely immersed in EM. These lamellae bearing CEC-like cells were cultured for 2wk. All

constructs were cultured in a carbon dioxide cell incubator containing 5% CO_2 at 37°C. The culture medium was exchanged every other day.

Uniaxial Tensile Testing for AAPCM and PAPCM
AAPCM, PAPCM and fresh pig corneas were cut into $10.0 \times 6.0 \text{ mm}^2$ rectangular strips along the longitudinal direction. The strips were then mounted under zero strain on to a purpose-built holder of an instron electromechanical universal tester (Instron, Canton, MA, USA). Uniaxial tensile testing was performed at a constant speed of 10 mm/min with a set load range from 0 to 500 g ($n=6$ in each group), as described by Oswal *et al*^[33]. All specimens maintained moist using physiological saline. All testing was performed at room temperature. One-way analysis of variance (ANOVA) was used to analyze the stress-strain curves derived from the specimens of each group. The value of statistical significance was set to $P < 0.05$ ($n=6$).

The Development of a Suspending Ring and MTT Cytotoxicity Assay
An acupuncture needle was heated in an alcohol flame until it softened and became wrinkled on a steel nail of 2 mm diameter, forming the shape of spring. Then the appearance was further changed to become a ring with a diameter of 8 mm and height of 2 mm (a suspending ring). To determine whether the soaking solutions from the suspending ring would cause cytotoxicity, the suspending ring was soaked using 5 mL EM at 37°C for 48h. Human corneal stromal (2×10^3) and epithelial (2×10^3) cells as well as CEC-like (2×10^3) cells were seeded into each well of 96-well plates and cultured with soaking solutions (experimental group, $n=6$) or normal medium (control group, $n=6$). MTT assay was used to determine the proliferation activity of the cells at 1, 3, 5, and 7d. A microplate reader (InTec Reader 2010, USA) was used to measured the optical density (OD) value of absorbance at 490 nm. Differences in the OD value between experimental and control groups were analyzed statistically by One-way ANOVA. The value of statistical significance was set to $P < 0.05$.

Construction of a Human Full-thickness Corneal Substitute
AAPCM lamellae were soaked in EM at 37°C for 24h before cell seeding. Cultured hCSCs from passage 3 were trypsinized, and re-suspended at a final concentration of 5×10^5 cells/mL. Parallel to the surface of the AAPCM lamellae, 1 mL of cell suspension was gently injected into the AAPCM stromal collagen at eight different sector regions using a 1 mL insulin syringe. The cell-AAPCM lamella constructs were incubated in carbon dioxide cell incubator containing 5% CO_2 at 37°C for 24h in order to reach the complete adhesion of the hCSCs to the AAPCM, and then they were cultured for the next 7d by the methods of shake culturing on an orbital shaker at a rotation rate of 15-20 rpm. After shake culturing for 7d, the human CECs from passage 1 were gently seeded onto the surface of the Bowman's membrane of the reconstructed

stroma with a cell density of $5 \times 10^3/\text{mm}^2$. The constructs kept still for 3h before being completely immersed in EM. The next day, the constructs were placed on the suspending rings with the constructed epithelium facing downwards in the wells of 48-well plates and CEC-like cells in 100 mL were gently seeded on the surface of the stoma at a density of 2×10^5 cells/ mm^2 for each construct, and allowed to adhere for 4h before being completely immersed in EM. After culturing for 1d, the constructs were turned over and cultured for 7d. When epithelial cells grown to reach confluence, the air-liquid culture technique was used for one more weeks for the construction of epithelium. All constructs were cultured in a carbon dioxide cell incubator containing 5% CO_2 at 37°C . The culture medium was exchanged every other day.

Immunofluorescent Staining Immunofluorescence was performed as previously reported^[34]. In brief, mouse monoclonal antibody for anti-cytokeratin 3 (CK3, 1:200; Abcam, San Francisco, CA, USA), a marker of CECs, anti-vimentin (1:100; Abcam, San Francisco, CA, USA), a marker of keratocytes, or anti- Na^+/K^+ ATPase alpha1 (1:50; Santa Cruz), expressed in the membrane of CECs, was placed on the sections and primary corneal cell cultures were fixed with 4% paraformaldehyde and incubated at 4°C overnight (PBS was the negative control). The secondary antibodies (1:100; all from Beijing Zhongshan) coupled to FITC or TRITC were then applied for detection, and the cells were stained with 4',6-diamidino-2-phenylindole (DAPI) to visualize nuclei. For negative controls, primary antibodies were substituted with PBS. Fluorescence was observed using a fluorescence microscope (models BH2-RFL-T3 and BX50; Olympus).

Histology Samples for scanning electron microscopy were fixed in cacodylate-buffered 3% glutaraldehyde and post-fixed for 1h in 1% osmium tetroxide. Then samples were gradually dehydrated by ethanol (50%, 70%, 95%, 100%), critical-point dried, and gold sputter-coated according to routine procedures^[35]. Subsequently, specimens were examined by a scanning electron microscope (SEM, S-570, Hitachi, Japan).

Implantation After being treated with antibiotic eyedrops three times a day for three days, male adult New Zealand White rabbits, weighing 2.0-2.5 kg, were anesthetized intravenously with 1% pentobarbital sodium (40-50 mg/kg) and topically with oxybuprocaine hydrochloride three times in half an hour, and the surgical eyes were disinfected and sterile draped. Next, full-thickness plant beds with a diameter of 7.5-mm were made on the central corneas of right eyes by trephine and then the prepared constructs were implanted onto it with 10-0 nylonsutures (Alcon). Subsequently, dexamethasone-tobramycin ointment (Santen) was instilled into the conjunctiva sac immediately.

Twenty rabbits were selected and randomly divided into two groups: the construct (rabbits with human full-depth corneal replacement transplantation, $n=10$) and AAPCM (rabbits with AAPCM lamellae transplantation, $n=10$). Tobramycin and dexamethasone eye drops were used 4 times and 1% cyclosporin one time each day during the follow-up period.

Follow-up Clinical Observations Conjunctival congestion, corneal edema, corneal neo-vascularization, and grafts degradation of each surgical eye ($n=20$) was examined by a slit-lamp microscope (Zeiss) 1, 3, 5, 7, 14, 21, and 28d after transplantation. Representative anterior segment photographs were made with a slit-lamp microscope. Central corneal thickness was measured at 1, 3, 5, 7, 14, 21, and 28d after surgery using a Visante OCT (Model CA94568; Carl Zeiss Meditec, Inc.). At 2wk after transplantation, the confocal microscope images of each surgical eye ($n=20$) were collected with confocal laser corneal microscopy.

RESULTS

Corneal Cells The dissociated human CECs attached well and grew extensively (Figure 1A), forming a continuous layer with a high expression of CK3 in the cytomembrane (Figure 1D). hCSCs had an elongated spindle-like shape and a good growth rate in culture (Figure 1B). Positive signals for vimentin were distributed throughout the cell plasma (Figure 1E). The CEC-like cells were hexagonal and pentagonal and grew to form a monolayer of cells (Figure 1C), characteristic of the morphology of normal human corneal endothelium. Positive signals for Na^+/K^+ ATPase were detected throughout the cytomembrane (Figure 1F).

Characterization of AAPCM and PAPCM

Microscopy and histology Gross observation of the AAPCM lamella (Figure 2A) and PAPCM lamella (Figure 2D) indicated they were opaque and swollen after the decellularization. However, their transparency was restored after being soaked in sterile glycerol for 1h (Figure 2B and 2E). Hematoxylin-eosin (H&E) staining indicated no visible cells or nuclear material in the AAPCM lamella (Figure 2C) or PAPCM lamella (Figure 2F), whereas collagen fibers, Bowman's membrane, and Descemet's membrane were retained and had a normal structure (Figure 2C and 2F). Bowman's membrane located on the anterior surface of AAPCM lamella had a smooth appearance (Figure 2A and 2B). The morphology of Descemet's membrane changed, becoming corrugated (Figure 2D and 2E).

Mechanical properties The mean \pm SD values for ultimate tensile strength were 4.75 ± 1.3499 MPa in the native porcine cornea, 4.45 ± 0.5398 MPa in the AAPCM, and 4.48 ± 0.9130 MPa in the PAPCM. No significant difference was found between the normal cornea, AAPCM, and PAPCM ($P > 0.05$; Figure 2G). The elongation at break (%) of the AAPCM was 6.05 ± 1.98 , similar to that of native porcine corneas (6.41 ± 2.52 , $P > 0.05$),

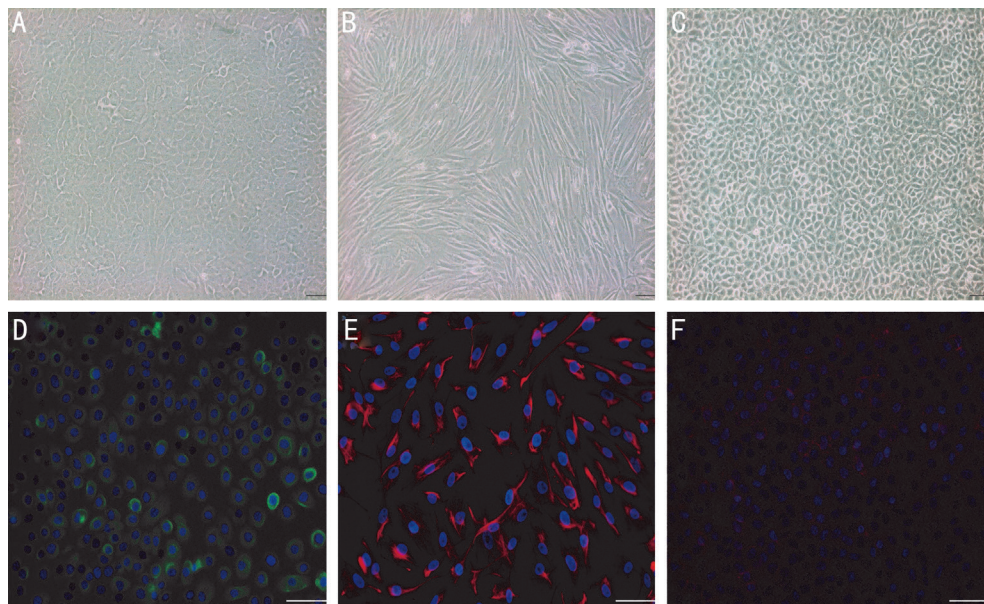


Figure 1 Corneal cells Dissociated human epithelial cells attached well and grew extensively (A) with a high expression of CK3 in the cytomembrane (D). Human stromal cells displayed an elongated spindle-like shape (B). Positive signals for vimentin were distributed in the cell plasma (E). CEC-like cells displayed a hexagonal and pentagonal shape (C). Positive signals for Na^+/K^+ ATPase were detected throughout the cytomembrane (F). Scale bars=20 μm .

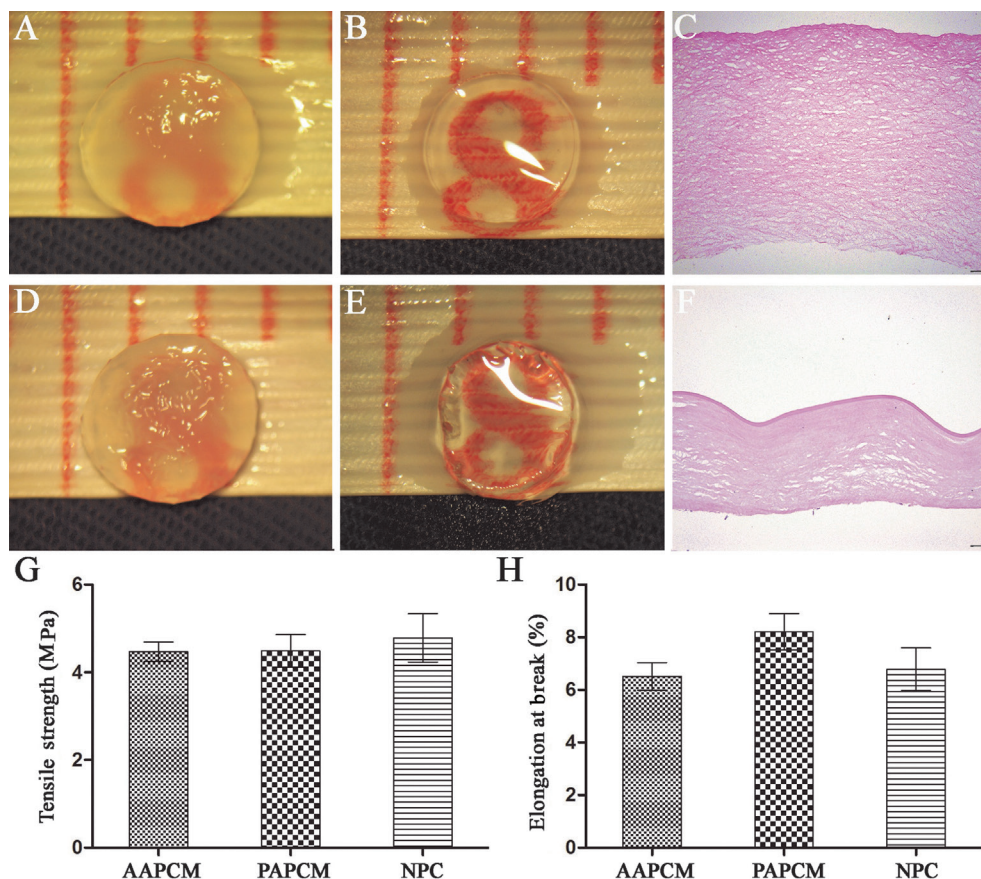


Figure 2 Representative images, histological characteristics and mechanical properties of the scaffolds AAPCM lamella (A) and PAPCM lamella (D) were opaque and swollen after decellularization by gross observation. Their transparency was restored after soaking in sterile glycerol for 1h (B, E). H&E staining indicated no visible cells or nuclear material in the AAPCM lamella (C) or PAPCM lamella (F). Bowman's membrane and Descemet's membrane were retained and had normal structures (C, F). Descemet's membrane was corrugated (D, E). Bowman's membrane had a smooth appearance (A, B). For ultimate tensile strength, no significant difference was found between the normal cornea, AAPCM, and PAPCM ($P>0.05$; G). There was a significant difference in the elongation at break between the PAPCM and normal cornea ($P<0.05$; H). Scale bars=20 μm . NPC: Native porcine cornea.

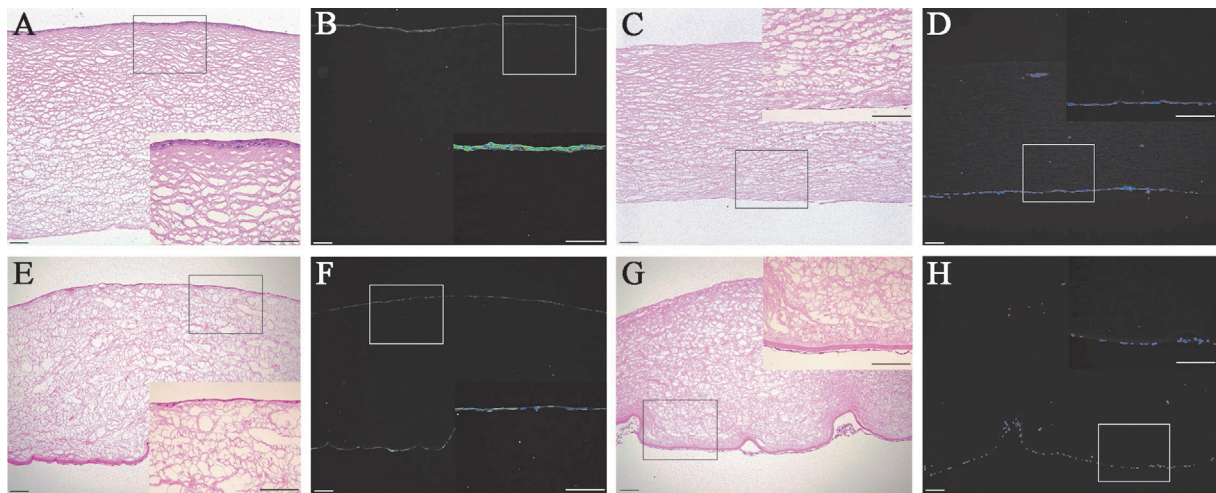


Figure 3 The reformulated corneal epithelium and endothelium Three or four layers of epithelial cells formed on the surface of Bowman's membrane of AAPCM (A), but there was only one layer of epithelial cells on the surface of PAPCM covering both the stromal and Descemet's membrane surface (E). Immunofluorescence showed these cells expressed CK3 (B, F). CEC-like cells formed an almost intact monolayer on the stromal surface of AAPCM and no cells were discovered within the AAPCM lamella (C). The CEC-like cells located on the corrugated Descemet's membrane of PAPCM showed a non-uniform monolayer with accumulation of many cells in the fold (G). These cells expressed Na^+/K^+ ATPase (D, H). Scale bars=20 μm .

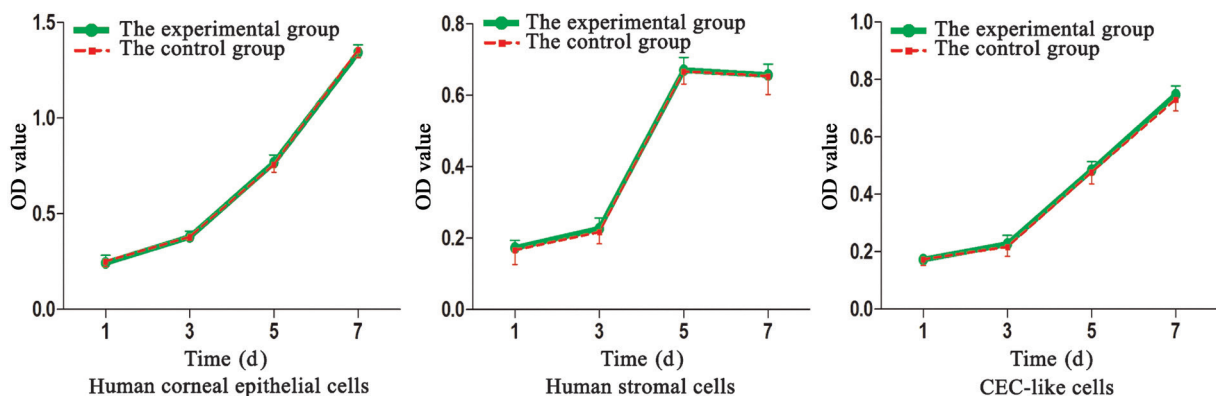


Figure 4 MTT assay for cytotoxicity determination of the soaking solutions from the suspending ring There were no significant differences in the proliferation of human corneal epithelial and stromal cells as well as CEC-like cells between the experimental and control groups ($P>0.05$).

and there was a significant difference in this value between the PAPCM (7.95 ± 2.37) and normal cornea ($P<0.05$; Figure 2H).

Morphology of the Reformulated Corneal Epithelium and Endothelium Three or four layers of epithelial cells with high expression of CK3 (Figure 3B) formed on the surface of Bowman's membrane of the AAPCM through the air-liquid culture technique (Figure 3A), but there was only one layer of epithelial cells on the surface of the PAPCM that covered the stromal and Descemet's membrane surface (Figure 3E), which also had a high expression of CK3 (Figure 3F). After 2wk of seeding, the CEC-like cells formed a nearly intact monolayer on the stromal surface of the AAPCM, and no cells were detected within the AAPCM lamella (Figure 3C). By immunofluorescence, these cells expressed Na^+/K^+ ATPase (Figure 3D). CEC-like cells on the corrugated Descemet's membrane of the PAPCM assumed a non-uniform monolayer, with many cells accumulating in the folds (Figure 3G) being positive for Na^+/K^+ ATPase (Figure 3H).

Cytotoxicity of the Suspending Ring MTT assay showed that the difference of cell proliferation was not statistically significant between the experimental and control groups ($n=6$, $P>0.05$; Figure 4).

Characterization of the Constructed Full-Depth Human Corneal Replacements Figure 5 shows the three-dimensional culture system (Figure 5B), composed of an acupuncture needle-devolved ring (Figure 5A) and the entire construct (Figure 5C). In the central stromal-like region, keratocytes were distributed uniformly throughout the AAPCM (Figure 5C) and expressed vimentin in the cell plasma (Figure 5E), demonstrating that human keratocytes survived and proliferated rapidly. On the surface of Bowman's membrane, the epithelial layer appeared as a thin, differentiated, stratified epithelium expressing CK3 in the cytomembrane (Figure 5D), which included three or four layers of cells but no column-shaped cells at the bottom (Figure 5C). On the lower surface, the endothelial monolayer was clearly visible as a line of

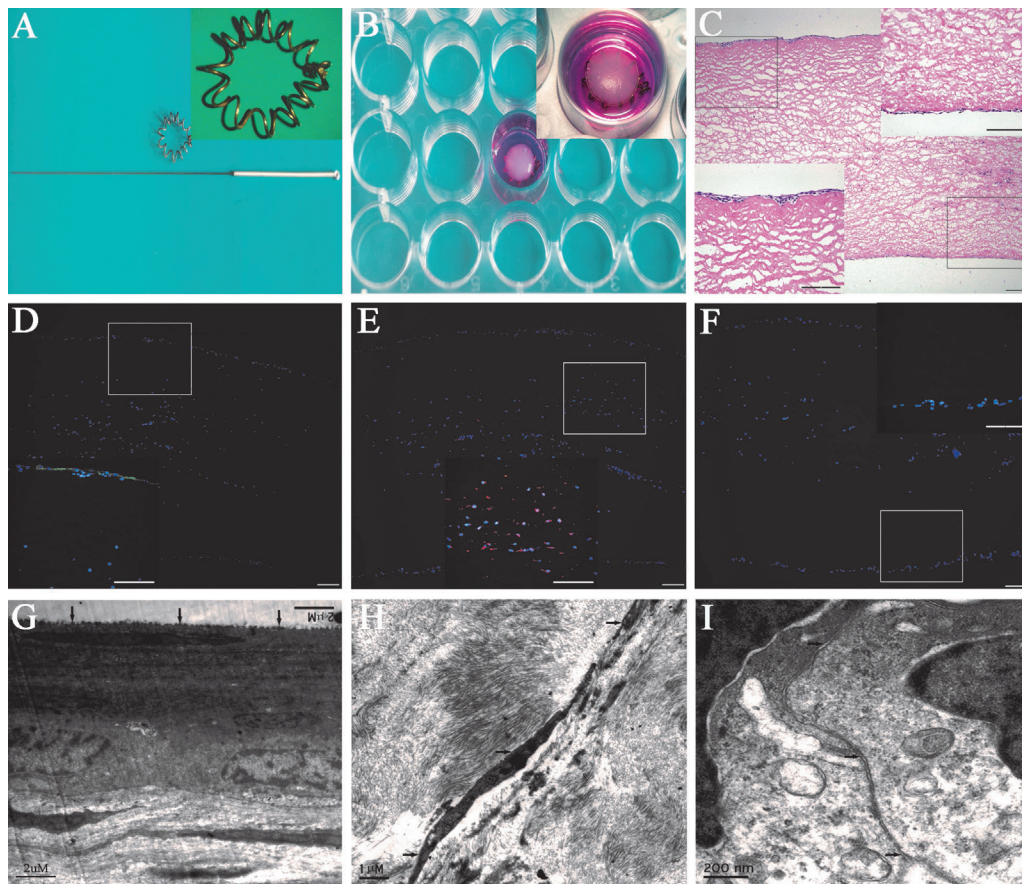


Figure 5 Representative images of the three-dimensional culture system and characteristics of human full-depth corneal replacements
 The suspending ring was derived from an acupuncture needle (A). The suspending ring located in the well of a 48-well plate lifted the construct, forming a three-dimensional culture system (B). In the central stromal-like region, keratocytes were distributed uniformly throughout the AAPCM (C) and expressed vimentin in the cell plasma (E). On the surface of Bowman's membrane, the epithelial layer included three or four layers of cells (C) expressing CK3 in the cytomembrane (D). On the lower surface, the endothelial monolayer was clearly visible as a line of cells (C) with the expression of Na⁺/K⁺ATPase in the cytomembrane (F). In contrast, Descemet's membrane was absent (C). Transmission electronic microscope demonstrated many microvilli on the epithelial cell surface (G), the long shuttle shape of stroma cell (H) and zonula occludens structure at the interface with endothelial cells (I). The images are local enlarged images. Scale bars=20 μm.

cells that expressed Na⁺/K⁺ATPase in the cytomembrane (Figure 5F). In contrast, Descemet's membrane, a structure that is easily viewed when present, was not observed as a thick collagenous layer by optical microscopy (Figure 5C). The construct was similar to normal human corneas, with many microvilli on the epithelial cell surface (Figure 5G), stromal cells with a long shuttle shape (Figure 5H), and zonula occludens at the interface with endothelial cells (Figure 5I), as demonstrated by transmission electron microscopy.

Implantation and Clinical Observations Figure 6 shows representative images throughout the entire operation. The transparency of the graft was restored gradually in the construct group (Figure 6A-6D), whereas it was always opaque and swollen in the AAPCM group (Figure 6E-6H).

Representative anterior segment photographs on a slit-lamp biomicroscope and Visante OCT were taken on postoperative days 3, 7, 14, and 28. The corneal transparency increased gradually and was nearly completely restored in the construct

group 7d after surgery (Figure 7A). However, corneal edema and conjunctiva congestion developed at 14d, indicating the occurrence of immune rejection, which deteriorated rapidly with neovascularization at 28d (Figure 7A). In contrast, the corneal opacity and stromal edema worsened throughout the 28-day observation in the PAPCM group (Figure 7B).

Confocal microscope images acquired 7d after the operation confirmed the uniform distribution of stromal cells in the stroma (Figure 8B) and the full coverage of polygonal cells on the posterior surface (Figure 8C) in the construct group, whereas no cells were detected in the stroma (Figure 8E), and the posterior surface was denuded (Figure 8F). The regenerated corneal epithelial cells on the implant surface in the construct group showed a more regular and intact morphology (Figure 8A) compared with the PAPCM group (Figure 8D).

DISCUSSION

The scaffold is a basic element in the construction of full-depth corneal replacements. Many researchers have demonstrated

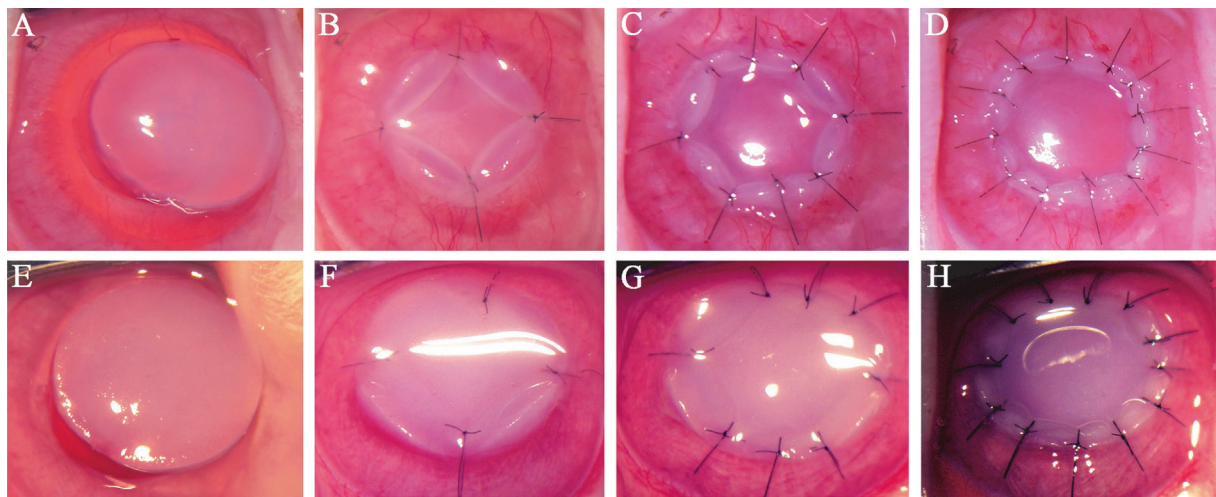


Figure 6 Representative images during the whole operation The transparency of the graft was restored gradually in the construct group (A, B, C, D), whereas it was always opaque and swollen in the AAPCM group (E, F, G, H).

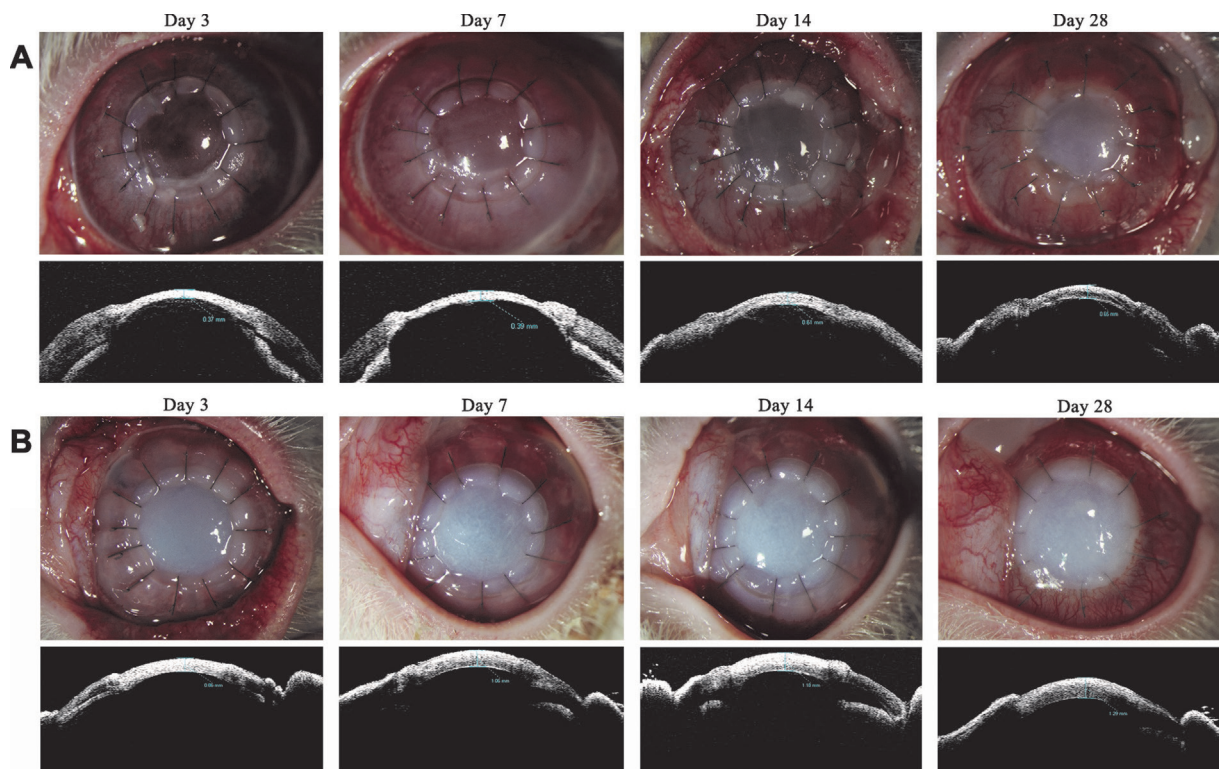


Figure 7 Observations after surgery. Representative anterior segment photographs made with a slit-lamp microscope (top row) and Visante OCT (bottom row) at different time points The corneal transparency was increased gradually and almost completely restored in the construct group 7d after surgery (A); however, the corneal edema and conjunctiva congestion appeared at 14d and deteriorated with the invasion of neovascularization at 28d (A). In contrast, the degree of corneal opacity and stromal edema was increasingly aggravated throughout the 28-day observation period in the PAPCM group (B).

that APCM is an ideal scaffold on the basis of its good optical clarity, biocompatibility and adequate biomechanical toughness. To date, no synthetic scaffolds have performed better than natural APCM at mimicking the structure of the natural corneal stroma with sufficiently good biomechanical properties to endure contact with sutures during keratoplasty. Recently, we constructed tissue-engineered epithelial grafts, anterior corneal replacements, and tissue-engineered corneal endothelial sheets with APCM and corneal cells. Furthermore,

we performed corneal stem cell transplantation, lamellar keratoplasty, and Descemet stripping automated endothelial keratoplasty using these constructs as implants in animal models^[29-31]. These constructs were tissue-engineered hemicorneas (*i.e.* anterior corneal replacements and posterior corneal replacements). Thus, the AAPCM was used as a scaffold for the construction of anterior corneal replacements versus the PAPCM for posterior corneal replacements, based on the corneal anatomy. However, it is unclear whether the

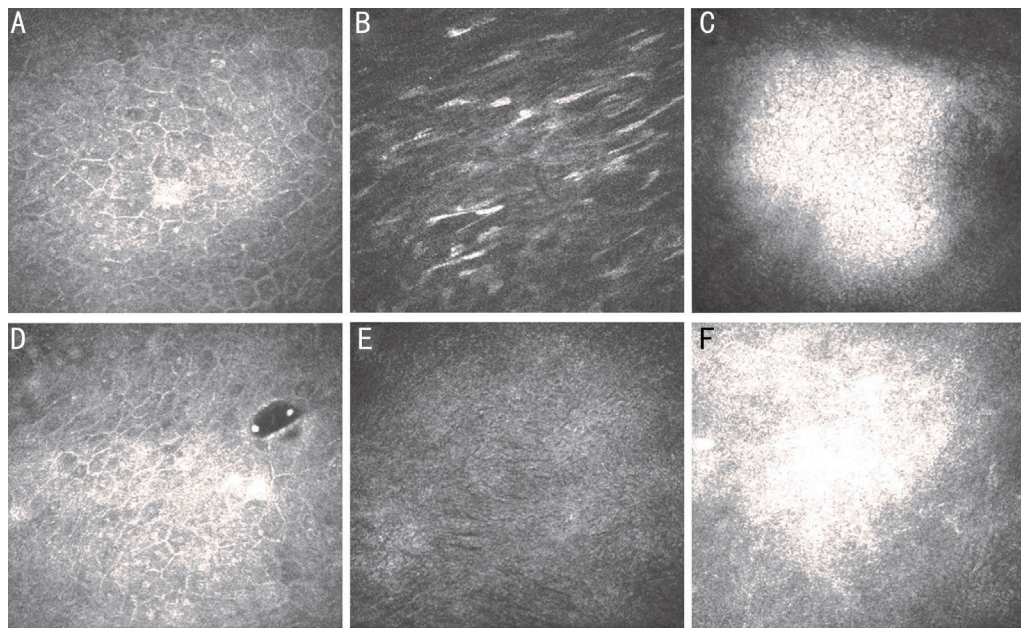


Figure 8 Confocal laser corneal microscopy images of corneal features in the construct group, alongside those in the PAPCM group, at 7d after construct implantation The confocal microscope images confirm the uniform distribution of stromal cells (B) and full coverage of the posterior surface by polygonal cells (C) in the construct group, whereas in the PAPCM group, the posterior surface was denuded (F) and no cells were detected in the stroma (E) in PAPCM group. The regenerated corneal epithelial cells on the implant surface of construct group showed a more regular and intact morphology (A) than in the PAPCM group (D).

AAPCM or PAPCM is the ideal scaffold for synthesizing full-depth corneal replacements.

In this study, we compared the properties of AAPCM and PAPCM to determine an appropriate scaffold for the construction of full-depth corneal replacements. Although the ultimate tensile strength of the PPACM was similar to that of the AAPCM, there was a significant difference in the elongation at break. In the control, the biomechanical property of the AAPCM was similar to that of the native porcine cornea versus the PAPCM.

There were also distinctions in the attachment and proliferation of corneal cells on the surfaces between the AAPCM and PAPCM in the construction of full-depth corneal replacements. The AAPCM retained an intact Bowman's membrane, which is the natural basement membrane of the corneal epithelium and which plays an important role in its maintenance^[36]. Our study demonstrated that the epithelium was thicker when grown on the Bowman's membrane of the AAPCM compared with the stromal surface of the PAPCM. Therefore, the AAPCM was better at stimulating the proliferation and differentiation of CECs compared with the PAPCM. Descemet's membrane is unique to the PAPCM.

Regarding corneal anatomy, the relationship between Descemet's membrane and the corneal endothelium is analogous to that between Bowman's membrane and the corneal epithelium. However, the endothelium that grew on Descemet's membrane of the PAPCM was a non-uniform monolayer, with many cells accumulating in the folds, which

was caused by edema that was unavoidable during the PAPCM preparation. In contrast, the stromal surface of the AAPCM was attached by a nearly intact and uniform monolayer, similar to normal endothelium. Thus, the AAPCM is the ideal scaffold for the construction of full-depth corneal replacements.

Enough corneal cells must be obtained for the construction of full-depth human corneal replacements. Corneal cells consist of three cell types: epithelial cells, stromal cells, and endothelial cells. CECs and stromal cells can regenerate *in vivo* and be cultured through many passages *in vitro*. However, human CECs do not normally divide *in vivo*, and the ability to proliferate is strictly limited *in vitro*^[37-40]. Fortunately, we have developed techniques to generate and purify CEC-like cells from hESCs, laying the foundation for the construction of full-depth human corneal replacements^[30].

We need to research and develop three-dimensional culture systems further to generate full-depth corneal replacements. Many researchers have developed full-depth human corneal replacements with the aid of porous culture inserts^[18,21-23]. These culture systems improve the construction of full-depth corneal replacements with synthetic polymer scaffolds, but they are unsuitable for the AAPCM. Unlike synthetic polymer scaffolds, which are in a liquid state in porous culture inserts when inoculated with CECs, the AAPCM remains solid throughout the entire construction.

Therefore, we designed a special suspending ring by changing the shape of an acupuncture needle and establishing a new three-dimensional organ culture system. Although the

acupuncture needle can be inserted into a patient's body at certain acupuncture points to treat diseases without toxicity, the MTT cytotoxicity assay is necessary for acupuncture needle-designed suspending rings, based on its prolonged contact with corneal cells during the construction of full-depth corneal replacements. The test results demonstrated that the soaking solution of the suspending ring had no effect on the culture of corneal cells. The suspending ring—with an outside diameter, inside diameter, and height of 8 mm, 4 mm, and 2 mm, respectively—was made to our specifications to meet the requirements of the three-dimensional culture system. The suspending ring lifted the construct through the points of contact between them in the wells of 48-well plates. Also, each contact point was small, because the suspending ring originated from an acupuncture needle, with a 0.20-mm in diameter. In this case, the construct was suspended in the culture medium, ensuring the three-dimensional co-culture of all three corneal cell types in different places throughout the same scaffold at the same time, generating full-depth human corneal replacements.

The proposed construct mimicked the three layers of the native human cornea. In this study, we demonstrated that the stratified epithelium attached well to Bowman's membrane of the construct and grew in three dimensions on its surface. Also, microvilli of the corneal epithelium were identified on the outermost cells, which play an important role in keeping the tear film stable and ocular surface healthy. However, the thickness of the epithelium of the construct was smaller than that of native corneas, and the cell type was relatively homogeneous, in contrast to the normal corneal epithelium, composed of basal cells and nonkeratinized, stratified squamous epithelial cells, although the air-lift culture model was introduced in this process.

The maintenance of normal corneal epithelium depends on limbal stem cells that reside in the limbus, and which self-renew with the potential to undergo multiple lines of differentiation^[41]. In our study, the epithelium of the construct originated from the seeded cells, which were obtained by culture, differentiation, and amplification of limbal epithelial cells *in vitro* and which lost their differentiation potential when they were inoculated. Thus, the structure of the epithelium between the construct and normal corneas is similar but not identical. We also found that a monolayer of CEC-like cells on the bottom surface of the construct formed the endothelium of the construct, with the same microstructure of zonula occludens and functional Na^+/K^+ ATPase as normal corneal endothelium.

The transparency of the construct was low because of edema caused by increasing collagen fibril spacing in the stroma after long-term culture *in vitro*, and this increased during the

operation but was completely restored 7d after the operation. AAPCM always showed edema and opacity either during the operation or after the operation. The transparency of the construct was significantly better than that of the AAPCM, which is surprising, and suggests that the construct was functional. However, it lacked Descemet's membranes. The absence of Descemet's membranes might be attributed to the short culture time in this system of the endothelial cells, which are responsible for the secretion of this layer^[42]. Moreover, the induction, differentiation, and subsequent culture of hESCs may affect the endothelial cell phenotype, which can influence secretion by Descemet's membrane.

Finally, the surface that was provided by the AAPCM was relatively rough, which may also affect endothelial cell secretion. Descemet's membrane is a corneal component, but it is not required for the maintenance of corneal transparency, as shown in our previous studies^[43]. The hCSCs survived in the construct but were dispersed primarily in the central region. This distribution was closely related to the seeding and culture methods that we adopted.

The inoculation caused the accumulation of cells in the central region of the construct in the first several days of construction. Moreover, the shift in the culture from shaking to static slowed the proliferation and spread of cells in the construct in the late period of construction, because the shaking culture strategy provided a dynamic system that improved cell growth by accelerating the exchange of waste. Although the distribution of keratocytes in the construct was not even, their morphology and function were preserved without differentiation into myofibroblasts, the key effector cells in scar-formation, as demonstrated by transmission electron microscopy, confocal microscopy, and slit-lamp biomicroscopy.

It is particularly important for corneal replacements to withstand the resistance of stitches in penetrating keratoplasty and the postoperative intraocular pressure, which should be addressed for their future clinical application. In our study, the construct withstood both factors. However, the construct triggered an acute and aggravating host immune response that destroyed it in this human/pig-to-rabbit xenotransplantation. This result is consistent with previous reports in which model corneal xenografts were rejected over 2-16d after transplantation in full-thickness murine corneal xenotransplantation^[44-46].

In contrast, no obvious immune rejection or complications related to the AAPCM graft were seen in the PAPCM group, demonstrating that the PAPCM scaffold has good biocompatibility and is non-immunogenic. It also suggests that the heterogenous cellular components in the construct were the primary cause of keratoplasty rejection episodes in the construct group. If monkeys were used as the recipients, the

immune rejection response to the construct graft would have been significantly reduced, because the genetic background is similar between monkeys and humans.

Future studies should use the stem cells as epithelium regeneration seeding cells, optimize keratocytes in the scaffold inoculation method, apply a dynamic culture environment throughout the construction, and introduce a femtosecond laser to obtain a smooth stroma cross-section to improve the structure of the construct and better simulate an actual cornea. Despite the need to refine the construction at each step and to improve the experimental animal model for penetrating keratoplasty, the constructs in this study had a similar morphology and ultrastructure to normal human corneas, especially with regard to their biomechanics, increasing their potential as substitutes for human donor corneal tissue for transplantation and rabbits in pharmacotoxicology testing.

ACKNOWLEDGEMENTS

We thank the Center of Reproductive Medicine, Shandong University for providing hESCs and its staff member Dr. Se-Xin Huang for technical support in culturing the cells. Thanks to Dr. Edward C. Mignot, formerly of Shandong University, for linguistic advice. We thank Edanz Group China (www.liwenbianji.cn/ac), for editing the English text of a draft of this manuscript.

Foundation: Supported by the Excellent Middle-aged and Yong Scientists Scientific Research Fund of Shandong Province, China (No.BS2014SW034).

Conflicts of Interest: Zhang K, None; Ren XX, None; Li P, None; Pang KP, None; Wang H, None.

REFERENCES

- 1 Fagerholm P, Lagali NS, Merrett K, Jackson WB, Munger R, Liu YW, Polarek JW, Söderqvist M, Griffith M. A biosynthetic alternative to human donor tissue for inducing corneal regeneration: 24-month follow-up of a phase I clinical study. *Sci Transl Med* 2010;2(46):46ra61.
- 2 Whitcher JP, Srinivasan M, Upadhyay MP. Corneal blindness: a global perspective. *Bull World Health Organ* 2001;79(3):214-221.
- 3 Matthaei M, Sandhaeger H, Hermel M, Adler W, Jun AS, Cursiefen C, Heindl LM. Changing indications in penetrating keratoplasty: a systematic review of 34 years of global reporting. *Transplantation* 2017;101(6):1387-1399.
- 4 Goweida MB. Intraoperative review of different bubble types formed during pneumodissection (big-bubble) deep anterior lamellar keratoplasty. *Cornea* 2015;34(6):621-624.
- 5 Arnalich-Montiel F, Alió Del Barrio JL, Alió JL. Corneal surgery in keratoconus: which type, which technique, which outcomes? *Eye Vis (Lond)* 2016;3:2.
- 6 Lagali N, Griffith M, Fagerholm P, Merrett K, Huynh M, Munger R. Innervation of tissue-engineered recombinant human collagen-based corneal substitutes: a comparative in vivo confocal microscopy study. *Invest Ophthalmol Vis Sci* 2008;49(9):3895-3902.

- 7 Dubord PJ, Evans GD, Macsai MS, Mannis MJ, Glasser DB, Strong DM, Noël L, Fehily D. Eye banking and corneal transplantation communicable adverse incidents: current status and project NOTIFY. *Cornea* 2013;32(8):1155-1166.

- 8 Hogan RN, Brown P, Heck E, Cavanagh HD. Risk of prion disease transmission from ocular donor tissue transplantation. *Cornea* 1999;18(1):2-11.

- 9 Armitage WJ, Tullo AB, Ironside JW. Risk of Creutzfeldt-Jakob disease transmission by ocular surgery and tissue transplantation. *Eye (Lond)* 2009;23(10):1926-1930.

- 10 Salvador-Culla B, Kolovou PE. Keratoprosthesis: A review of recent advances in the field. *J Funct Biomater* 2016;7(2):E13.

- 11 Wilhelmus KR. The draize eye test. *Surv Ophthalmol* 2001;45(6):493-515.

- 12 Torricelli AA, Singh V, Santhiago MR, Wilson SE. The corneal epithelial basement membrane: structure, function, and disease. *Invest Ophthalmol Vis Sci* 2013;54(9):6390-6400.

- 13 Meller D, Peters K, Meller K. Human cornea and sclera studied by atomic force microscopy. *Cell Tissue Res* 1997;288(1):111-118.

- 14 Freegard TJ. The physical basis of transparency of the normal cornea. *Eye (Lond)* 1997;11(Pt 4):465-471.

- 15 DelMonte DW, Kim T. Anatomy and physiology of the cornea. *J Cataract Refract Surg* 2011;37(3):588-598.

- 16 van Susante JLC, Piepe J, Buma P, van Kuppevelt TH, van Beuningen H, van Der Kraan PM, Veerkamp JH, van den Berg WB, Veth RPH. Linkage of chondroitin-sulfate to type I collagen scaffolds stimulates the bioactivity of seeded chondrocytes *in vitro*. *Biomaterials* 2001;22(17):2359-2369.

- 17 Luo HL, Lu YB, Wu TT, Zhang M, Zhang YJ, Jin Y. Construction of tissue-engineered cornea composed of amniotic epithelial cells and acellular porcine cornea for treating corneal alkali burn. *Biomaterials* 2013;34(28):6748-6759.

- 18 Griffith M, Osborne R, Munger R, Xiong X, Doillon CJ, Laycock NL, Hakim M, Song Y, Watsky MA. Functional human corneal equivalents constructed from cell lines. *Science* 1999;286(5447):2169-2172.

- 19 Alaminos M, Del Carmen Sánchez-Quevedo M, Muñoz-Avila JI, Serrano D, Medialdea S, Carreras I, Campos A. Construction of a complete rabbit cornea substitute using a fibrin-agarose scaffold. *Invest Ophthalmol Vis Sci* 2006;47(8):3311-3317.

- 20 Bonanno JA. Identity and regulation of ion transport mechanisms in the corneal endothelium. *Prog Retin Eye Res* 2003;22(1):69-94.

- 21 Zhang ZH, Niu GG, Choi JS, Giegengack M, Atala A, Soker S. Bioengineered multilayered human corneas from discarded human corneal tissue. *Biomed Mater* 2015;10(3):035012.

- 22 Orwin EJ, Hubel A. In vitro culture characteristics of corneal epithelial, endothelial, and keratocyte cells in a native collagen matrix. *Tissue Eng* 2000;6(4):307-319.

- 23 Vrana NE, Builles N, Justin V, Bednarz J, Pellegrini G, Ferrari B, Damour O, Hulmes DJ, Hasirci V. Development of a reconstructed cornea from collagen-chondroitin sulfate foams and human cell cultures. *Invest Ophthalmol Vis Sci* 2008;49(12):5325-5331.

- 24 Builles N, Bechetoille N, Justin V, André V, Barbaro V, Di Iorio E, Auxenfans C, Hulmes DJ, Damour O. Development of a hemicornea from human primary cell cultures for pharmacotoxicology testing. *Cell Biol Toxicol* 2007;23(4):279-292.
- 25 Ide T, Nishida K, Yamato M, Sumide T, Utsumi M, Nozaki T, Kikuchi A, Okano T, Tano Y. Structural characterization of bioengineered human corneal endothelial cell sheets fabricated on temperature-responsive culture dishes. *Biomaterials* 2006;27(4):607-614.
- 26 Torbet J, Malbouyres M, Builles N, Justin V, Roulet M, Damour O, Oldberg A, Ruggiero F, Hulmes DJ. Orthogonal scaffold of magnetically aligned collagen lamellae for corneal stroma reconstruction. *Biomaterials* 2007;28(29):4268-4276.
- 27 Couture C, Zaniolo K, Carrier P, Lake J, Patenaude J, Germain L, Guérin SL. The tissue-engineered human cornea as a model to study expression of matrix metalloproteinases during corneal wound healing. *Biomaterials* 2016;78:86-101.
- 28 Du LQ, Wu XY, Pang KP, Yang YM. Histological evaluation and biomechanical characterisation of an acellular porcine cornea scaffold. *Br J Ophthalmol* 2011;95(3):410-414.
- 29 Zhu J, Zhang K, Sun Y, Gao X, Li YC, Chen ZJ, Wu XY. Reconstruction of functional ocular surface by acellular porcine cornea matrix scaffold and limbal stem cells derived from human embryonic stem cells. *Tissue Eng Part A* 2013;19(21-22):2412-2425.
- 30 Zhang K, Pang KP, Wu XY. Isolation and transplantation of corneal endothelial cell-like cells derived from in-vitro-differentiated human embryonic stem cells. *Stem Cells Dev* 2014;23(12):1340-1354.
- 31 Pang KP, Du LQ, Wu XY. A rabbit anterior cornea replacement derived from acellular porcine cornea matrix, epithelial cells and keratocytes. *Biomaterials* 2010;31(28):7257-7265.
- 32 Pang KP, Du LQ, Zhang K, Dai CY, Ju CQ, Zhu J, Wu XY. Three-dimensional construction of a rabbit anterior corneal replacement for lamellar keratoplasty. *PLoS One* 2016;11(12):e0168084.
- 33 Oswal D, Korossis S, Mirsadraee S, Wilcox H, Watterson K, Fisher J, Ingham E. Biomechanical characterization of decellularized and cross-linked bovine pericardium. *J Heart Valve Dis* 2007;16(2):165-174.
- 34 Chen Z, de Paiva CS, Luo LH, Kretzer FL, Pflugfelder SC, Li DQ. Characterization of putative stem cell phenotype in human limbal epithelia. *Stem Cells* 2004;22(3):355-366.
- 35 Sánchez-Quevedo MC, Moreu G, Campos A, García JM, González-Jaranay M. Regional differences in cell surface patterns in normal human sulcular epithelium. *Histol Histopathol* 1994;9(1):149-153.
- 36 Wilson SE, Liu JJ, Mohan RR. Stromal-epithelial interactions in the cornea. *Prog Retin Eye Res* 1999;18(3):293-309.
- 37 Ljubimov AV, Saghizadeh M. Progress in corneal wound healing. *Prog Retin Eye Res* 2015;49:17-45.
- 38 Hollingsworth J, I Perez-Gomez, HA Mutalib, N Efron. A population study of the normal cornea using anin vivo, slit-scanning confocal microscope. *Optom Vis Sci* 2001;78(10):706-711.
- 39 Joyce NC, Harris DL, Mello DM. Mechanisms of mitotic inhibition in corneal endothelium: contact inhibition and TGF-beta2. *Invest Ophthalmol Vis Sci* 2002;43(7):2152-2159.
- 40 Yuan S, Fan G. Stem cell-based therapy of corneal epithelial and endothelial diseases. *Regen Med* 2015;10:495-504.
- 41 Dua HS, Azuara-Blanco A. Limbal stem cells of the corneal epithelium. *Surv Ophthalmol* 2000;44(5):415-425.
- 42 Nishimura T, Toda S, Mitsumoto T, Oono S, Sugihara H. Effects of hepatocyte growth factor, transforming growth factor-beta1 and epidermal growth factor on bovine corneal epithelial cells under epithelial-keratocyte interaction in reconstruction culture. *Exp Eye Res* 1998;66(1):105-116.
- 43 Ju CQ, Zhang K, Wu XY. Derivation of corneal endothelial cell-like cells from rat neural crest cells in vitro. *PLoS One* 2012;7(7):e42378.
- 44 Ross JR, Howell DN, Sanfilippo FP. Characteristics of corneal xenograft rejection in a discordant species combination. *Invest Ophthalmol Vis Sci* 1993;34(8):2469-2476.
- 45 Yamagami S, Isobe M, Yamagami H, Hori J, Tsuru T. Mechanism of concordant corneal xenograft rejection in mice: synergistic effects of anti-leukocyte function-associated antigen-1 monoclonal antibody and FK₅₀₆. *Transplantation* 1997;64(1):42-48.
- 46 Tanaka K, Yamada J, Streilein JW. Xenoreactive CD4+ T cells and acute rejection of orthotopic guinea pig corneas in mice. *Invest Ophthalmol Vis Sci* 2000;41(7):1827-1832.